Exotic fully heavy $Q\bar{Q}Q\bar{Q}$ tetraquark states in $\mathbf{8}_{[Q\bar{Q}]} \otimes \mathbf{8}_{[Q\bar{Q}]}$ color configuration

Qi-Nan Wang, Zi-Yan Yang, and Wei Chen*

School of Physics, Sun Yat-Sen University, Guangzhou 510275, China

(Received 18 September 2021; accepted 10 December 2021; published 28 December 2021)

We have systematically calculated the mass spectra for S-wave and P-wave fully charm $c\bar{c}c\bar{c}$ and fully bottom $b\bar{b}b\bar{b}$ tetraquark states in the $\mathbf{8}_{[Q\bar{Q}]} \otimes \mathbf{8}_{[Q\bar{Q}]}$ color configuration, by using the moment QCD sum rule method. The masses for the fully charm $c\bar{c}c\bar{c}$ tetraquark states are predicted about 6.3–6.5 GeV for S-wave channels and 7.0–7.2 GeV for P-wave channels. These results suggest the possibility that there are some $\mathbf{8}_{[c\bar{c}]} \otimes \mathbf{8}_{[c\bar{c}]}$ components in LHCb's di-J/ψ structures. For the fully bottom $b\bar{b}b\bar{b}$ system, their masses are calculated around 18.2 GeV for S-wave tetraquark states while 18.4–18.8 GeV for P-wave ones, which are below the $\eta_b\eta_b$ and $\Upsilon(1S)\Upsilon(1S)$ two-meson decay thresholds.

DOI: 10.1103/PhysRevD.104.114037

I. INTRODUCTION

The existence of multiquark states was first suggested by Gell-Mann and Zweig at the birth of the quark model [1,2]. Since 2003, plenty of charmoniumlike exotic states and P_c states have been observed [3–12], many of which are unexpected and cannot be fitted into the conventional quark model. To understand the nature of these new resonances, many exotic hadron configurations have been proposed such as hadron molecules, compact multiquarks, hybrid mesons, and so on [13–18]. Among these theoretical models, the loosely bound hadron molecule and compact multiquark are two especially appealing configurations. For the charmoniumlike XYZ and P_c states, it is complicated and difficult to distinguish these two different hadron configurations experimentally and theoretically because of the existence of light quarks.

In 2017, an exotic structure around 18.4 GeV was reported by the CMS Collaboration in the $\Upsilon(1S)\mu^+\mu^-$ channel [19], which was once regarded as a fully bottom $bb\bar{b}\bar{b}$ tetraquark state. In 2019, the ANDY Collaboration at RHIC reported evidence of a significance peak at around 18.12 GeV [20]. Although these structures were not confirmed by some other experiments [21,22], their observations still attracted a lot of research interest in fully heavy tetraquark states [23–32]. Very recently, the LHCb Collaboration declared a narrow resonance $X(6900)$ in the di-$J\psi$ mass spectrum with a significance of more than 5σ [33]. Moreover, a broad structure ranging from 6.2 to 6.8 GeV and a hint for another structure around 7.2 GeV were also reported at the same time [33]. These exotic structures observed in LHCb immediately attracted great attention to study the fully charm $cc\bar{c}\bar{c}$ tetraquarks for their mass spectra [34–61], their production mechanisms [57,62–71], and their decay properties [37,46,72–75]. Because of the absence of light quarks, a fully heavy tetraquark system is more likely to form a compact tetraquark state via the gluon-exchange color interaction rather than a loosely hadron molecule combined by the light meson exchanged interaction [76,77].

Nevertheless, the authors of Ref. [78] discussed the interaction between two J/ψ mesons via the exchange of soft gluons, which hadronize into two light mesons at large distance. By studying the correlated $\pi\pi$ and $K\bar{K}$ exchanges, they found that it is possible for two J/ψ mesons to form a bound state. In Ref. [34], the authors studied the dicharmonia states in $\mathbf{1}_{[c\bar{c}]} \otimes \mathbf{1}_{[c\bar{c}]}$ configuration with $J^{PC} = 0^{++}$ and predicted their masses around 6.0–6.7 GeV in the method of QCD sum rules. The existence of dicharmonia bound states was also studied in Ref. [61], in which the authors investigated the $\eta_c\eta_c$, $J/\psi J/\psi$ bound states in both $\mathbf{1}_{[c\bar{c}]} \otimes \mathbf{1}_{[c\bar{c}]}$ and $\mathbf{8}_{[c\bar{c}]} \otimes \mathbf{8}_{[c\bar{c}]}$ color structures by using a nonrelativistic quark model. The 0^{++} dicharmonia states in the $\mathbf{8}_{[c\bar{c}]} \otimes \mathbf{8}_{[c\bar{c}]}$ color structure were also investigated in Ref. [54] by the Laplace QCD sum rule method.

In our previous works in Refs. [23,79,80], we have studied the fully heavy tetraquark states in diquark-antidiquark configuration with both $\mathbf{6}_{[QQ]} \otimes \bar{\mathbf{6}}_{[\bar{Q}\bar{Q}]}$ and $\bar{\mathbf{3}}_{[QQ]} \otimes \mathbf{3}_{[\bar{Q}\bar{Q}]}$ color structures. In this work, we shall further investigate the possibility of fully heavy tetraquark states in meson-meson configuration with $\mathbf{8}_{[Q\bar{Q}]} \otimes \mathbf{8}_{[Q\bar{Q}]}$ color

*chenwei29@mail.sysu.edu.cn

structure by using the method of QCD moment sum rules [81,82].

This paper is organized as follows. In Sec. II, we construct the interpolating currents for $\mathbf{8}_{[Q\bar{Q}]}\otimes\mathbf{8}_{[Q\bar{Q}]}$ meson-meson tetraquark states. In Sec. III, we evaluate the correlation functions for these interpolating currents. We extract the masses for these tetraquark states by performing the moment QCD sum rule analyses in Sec. IV. The last section is a brief summary.

II. INTERPOLATING CURRENTS

The color structure of a meson-meson operator $[Q\bar{Q}][Q\bar{Q}]$ can be written via the SU(3) symmetry

$$
\begin{aligned}
&(\mathbf{3}\otimes\bar{\mathbf{3}})_{[Q\bar{Q}]}\otimes(\mathbf{3}\otimes\bar{\mathbf{3}})_{[Q\bar{Q}]}\\
&\quad=(\mathbf{1}\oplus\mathbf{8})_{[Q\bar{Q}]}\otimes(\mathbf{1}\oplus\mathbf{8})_{[Q\bar{Q}]}\\
&\quad=(\mathbf{1}\otimes\mathbf{1})\oplus(\mathbf{1}\otimes\mathbf{8})\oplus(\mathbf{8}\otimes\mathbf{1})\oplus(\mathbf{8}\otimes\mathbf{8})\\
&\quad=\mathbf{1}\oplus\mathbf{8}\oplus\mathbf{8}\oplus(\mathbf{1}\oplus\mathbf{8}\oplus\mathbf{8}\oplus\mathbf{10}\oplus\overline{\mathbf{10}}\oplus\mathbf{27}), \qquad (1)
\end{aligned}
$$

in which the color singlet structures come from the $(\mathbf{1}_{[Q\bar{Q}]}\otimes\mathbf{1}_{[Q\bar{Q}]})$ and $(\mathbf{8}_{[Q\bar{Q}]}\otimes\mathbf{8}_{[Q\bar{Q}]})$ terms. Following Ref. [83], we can construct the S-wave and P-wave $[Q\bar{Q}][Q\bar{Q}]$ interpolating currents as below.

(i) The S-wave interpolating currents are

$$
\begin{aligned}
J^{PC}=0^{++}:\ J_1&=(\bar{Q}_a\gamma_5\lambda^n_{ab}Q_b)(\bar{Q}_d\gamma_5\lambda^n_{de}Q_e),\\
J_2&=(\bar{Q}_a\gamma_\mu\lambda^n_{ab}Q_b)(\bar{Q}_d\gamma_\mu\lambda^n_{de}Q_e),\\
J^{PC}=1^{+-}:\ J_{1\mu}&=(\bar{Q}_a\gamma_\mu\lambda^n_{ab}Q_b)(\bar{Q}_d\gamma_5\lambda^n_{de}Q_e),\\
J^{PC}=2^{++},0^{++}:\ J_{\mu\nu}&=(\bar{Q}_a\gamma_\mu\lambda^n_{ab}Q_b)(\bar{Q}_d\gamma_\nu\lambda^n_{de}Q_e),
\end{aligned}
\qquad (2)
$$

in which we obtain only $[Q\bar{Q}][Q\bar{Q}]$ currents with $J^{PC}=0^{++}$, 1^{+-}, and 2^{++} in the S-wave channel. The tensor current $J_{\mu\nu}$ can couple to both the $J^{PC}=0^{++}$ and 2^{++} quantum numbers but not the $J^{PC}=1^{++}$ channel because of the Lorentz symmetry restriction.

(ii) The P-wave interpolating currents are

$$
\begin{aligned}
J^{PC}=0^{-+}:\ \eta_1&=(\bar{Q}_a\gamma_5\lambda^n_{ab}Q_b)(\bar{Q}_d\lambda^n_{de}Q_e),\\
\eta_2&=(\bar{Q}_a\sigma_{\mu\nu}\lambda^n_{ab}Q_b)(\bar{Q}_d\sigma_{\mu\nu}\gamma_5\lambda^n_{de}Q_e),\\
J^{PC}=0^{--}:\ \eta_3&=(\bar{Q}_a\gamma_\mu\lambda^n_{ab}Q_b)(\bar{Q}_d\gamma_\mu\gamma_5\lambda^n_{de}Q_e),\\
J^{PC}=1^{--}:\ \eta_{1\mu}&=(\bar{Q}_a\gamma_\mu\lambda^n_{ab}Q_b)(\bar{Q}_d\lambda^n_{de}Q_e),\\
\eta_{2\mu}&=(\bar{Q}_a\gamma_\alpha\gamma_5\lambda^n_{ab}Q_b)(\bar{Q}_d\sigma_{\alpha\mu}\gamma_5\lambda^n_{de}Q_e),\\
J^{PC}=1^{-+}:\ \eta_{3\mu}&=(\bar{Q}_a\gamma_5\lambda^n_{ab}Q_b)(\bar{Q}_d\gamma_\mu\gamma_5\lambda^n_{de}Q_e),\\
\eta_{4\mu}&=(\bar{Q}_a\gamma_\mu\lambda^n_{ab}Q_b)(\bar{Q}_d\sigma_{\mu\nu}\lambda^n_{de}Q_e), \qquad (3)
\end{aligned}
$$

where only one P-wave $[Q\bar{Q}]$ operator is contained in these interpolating currents. One should note that these tetraquark interpolating currents with $\mathbf{8}_{[Q\bar{Q}]}\otimes\mathbf{8}_{[Q\bar{Q}]}$ color structure can be written as combinations of the diquark-antidiquark operators through the Fierz transformation and the color rearrangement. Their decay properties should be the same with the $[QQ][\bar{Q}\bar{Q}]$ tetraquark states as discussed in Refs. [23,74]. Thus, we shall not discuss the decay behaviors for these $[Q\bar{Q}][Q\bar{Q}]$ tetraquarks in this work.

III. QCD SUM RULES

In this section, we investigate the two-point correlation functions of the interpolating currents constructed above. For the scalar and pseudoscalar currents, the correlation functions are

$$
\Pi(p^2)=i\int d^4x e^{ip\cdot x}\langle 0|T[J(x)J^\dagger(0)]|0\rangle, \qquad (4)
$$

while for the vector and axial-vector currents

$$
\Pi_{\mu\nu}(p^2)=i\int d^4x e^{ip\cdot x}\langle 0|T[J_\mu(x)J_\nu^\dagger(0)]|0\rangle. \qquad (5)
$$

The correlation function $\Pi_{\mu\nu}(p^2)$ in Eq. (5) can be divided into two parts:

$$
\Pi_{\mu\nu}(p^2)=\left(\frac{p_\mu p_\nu}{p^2}-g_{\mu\nu}\right)\Pi_1(p^2)+\frac{p_\mu p_\nu}{p^2}\Pi_0(p^2), \qquad (6)
$$

where $\Pi_0(p^2)$ and $\Pi_1(p^2)$ represent the spin-0 and spin-1 invariant functions, respectively. For the tensor currents $J_{\mu\nu}(x)$ in Eq. (2),

$$
\Pi_{\mu\nu,\rho\sigma}(p^2)=i\int d^4x e^{ip\cdot x}\langle 0|T[J_{\mu\nu}(x)J_{\rho\sigma}^\dagger(0)]|0\rangle. \qquad (7)
$$

The correlation function $\Pi_{\mu\nu,\rho\sigma}(p^2)$ in Eq. (7) can be expressed as

$$
\Pi_{\mu\nu,\rho\sigma}(p^2)=\left(\eta_{\mu\rho}\eta_{\nu\sigma}+\eta_{\mu\sigma}\eta_{\nu\rho}-\frac{2}{3}\eta_{\mu\nu}\eta_{\rho\sigma}\right)\Pi_2(p^2)+\cdots, \qquad (8)
$$

where

$$
\eta_{\mu\nu}=\frac{p_\mu p_\nu}{p^2}-g_{\mu\nu}. \qquad (9)
$$

The invariant function $\Pi_2(p^2)$ relates to the spin-2 intermediate state, and the "$\cdots$" represents the contributions from other states.

At the hadron level, the invariant functions can be expressed through the dispersion relation

$$\Pi(p^2) = \frac{(p^2)^N}{\pi}\int_{16m_Q^2}^{\infty}\frac{\mathrm{Im}\Pi(s)}{s^N(s-p^2-i\epsilon)}ds + \sum_{n=0}^{N-1} b_n(p^2)^n, \tag{10}$$

where b_n is the subtraction constant. In QCD sum rules, the imaginary parts of the correlation functions are usually simplified as the following "pole plus continuum" spectral function:

$$\begin{aligned}\rho(s) &= \frac{1}{\pi}\mathrm{Im}\Pi(s)\\ &= f_H^2\delta(s-m_H^2)\\ &\quad + \text{QCD continuum and higher states},\end{aligned} \tag{11}$$

in which the δ function represents the lowest-lying state. The parameters f_H and m_H are the coupling constant and mass of the lowest-lying hadronic resonance H, respectively:

$$\begin{aligned}\langle 0|J|H\rangle &= f_H,\\ \langle 0|J_\mu|H\rangle &= f_H\epsilon_\mu,\\ \langle 0|J_{\mu\nu}|H\rangle &= f_H\epsilon_{\mu\nu},\end{aligned} \tag{12}$$

with the polarization vector ϵ_μ and polarization tensor $\epsilon_{\mu\nu}$.

To extract the lowest-lying resonance, we first define the moments by taking derivatives of the correlation function $\Pi(q^2)$ in Euclidean region $Q^2 = -q^2 > 0$:

$$\begin{aligned}M_n(Q_0^2) &= \frac{1}{n!}\left(-\frac{d}{dQ^2}\right)^n \Pi(Q^2)\Big|_{Q^2=Q_0^2}\\ &= \int_{16m_Q^2}^{\infty}\frac{\rho(s)}{(s+Q_0^2)^{n+1}}ds.\end{aligned} \tag{13}$$

We then rewrite the moments by applying the above equation to Eq. (10) and obtain

$$M_n(Q_0^2) = \frac{f_H^2}{(m_H^2+Q_0^2)^{n+1}}[1+\delta_n(Q_0^2)], \tag{14}$$

where $\delta_n(Q_0^2)$ represents higher excited states and continuum contribution, and it is a function of n and Q_0^2. It should be noted that, for a specific value of Q_0^2, $\delta_n(Q_0^2)$ will tend to zero as n going to infinity. Considering the ratio of the moments to remove the unknown coupling constant f_H

$$r(n,Q_0^2) \equiv \frac{M_n(Q_0^2)}{M_{n+1}(Q_0^2)} = (m_H^2+Q_0^2)\frac{1+\delta_n(Q_0^2)}{1+\delta_{n+1}(Q_0^2)}, \tag{15}$$

where the relation $\delta_n(Q_0^2) \approx \delta_{n+1}(Q_0^2)$ will be satisfied when n is large enough, we can extract the hadron mass as

$$m_H = \sqrt{r(n,Q_0^2) - Q_0^2}. \tag{16}$$

At the quark-gluon level, we can evaluate the invariant functions $\Pi(p^2)$ via the operator product expansion (OPE) method. The Wilson coefficients can be calculated by adopting the following heavy quark propagator in momentum space:

$$\begin{aligned}iS_Q^{ab}(p) =& \frac{i\delta^{ab}}{\hat{p}-m_Q} + \frac{i}{4}g_s\frac{\lambda_{ab}^n}{2}G_{\mu\nu}^n\frac{\sigma^{\mu\nu}(\hat{p}+m_Q)+(\hat{p}+m_Q)\sigma^{\mu\nu}}{12}\\ &+ \frac{i\delta^{ab}}{12}\langle g_s^2GG\rangle m_Q\frac{p^2+m_Q\hat{p}}{(p^2-m_Q^2)^4},\end{aligned} \tag{17}$$

where Q represents the charm quark or bottom quark field. The superscripts a, b are the color indices and $\hat{p} = p^\mu\gamma_\mu$. In this work, we will evaluate only the perturbative term and gluon condensate term in the correlation function; the contributions from higher nonperturbative terms such as the trigluon condensate are small enough to be neglected.

IV. NUMERICAL ANALYSIS

We now perform the QCD moment sum rule analyses by adopting the following values of heavy quark masses and gluon condensate [84–86]:

$$\begin{aligned}m_c(m_c) &= (1.27^{+0.02}_{-0.02})\ \mathrm{GeV},\\ m_b(m_b) &= (4.18^{+0.03}_{-0.02})\ \mathrm{GeV},\\ \langle g_s^2GG\rangle &= (0.88\pm 0.25)\ \mathrm{GeV}^4.\end{aligned} \tag{18}$$

As mentioned in Sec. III, there remain two important parameters n and Q_0^2 in the extracted hadron mass in Eq. (16). In the original literature on moment sum rules, the authors set $Q_0^2 = 0$, which may lead to a bad OPE convergence. To avoid such bad behavior, we follow Refs. [23,79,80] to choose $Q_0^2 > 0$ and introduce $\xi = Q_0^2/(4m_c)^2$ to perform sum rule analysis. The parameters n and ξ are related to each other through the following respects: (i) A large enough n will reduce the higher excited states and continuum region contributions, but it will also decrease the convergence of OPE series. (ii) A large ξ (or Q_0^2) can compensate the OPE convergence (see Fig. 1) but may cause a bad convergence of $\delta_n(Q_0^2)$ and make it difficult to obtain the parameters of the lowest-lying resonance. One needs to find suitable working regions for these two parameters to establish stable sum rules.

We take the interpolating current $J_1(x)$ with $J^{PC} = 0^{++}$ as an example to show the numerical analysis details. The correlation function of this current is evaluated as the following:

$$
\begin{aligned}
\Pi^{\mathrm{pert}}(Q^2) =& \frac{1}{192\pi^6}\int_0^1 dx\int_0^1 dy\int_0^1 dz\Bigg\{\left(\frac{-13x(1-x)y(1-y)^3(1-z)}{z^3}\right)F(m_c,Q^2)^4+\Bigg(\frac{40m_c^2y(1-y)}{z^2}\\
&-\frac{52Q^2x(1-x)y(1-y)^3(1-z)^2}{z^2}\Bigg)F(m_c,Q^2)^3+\Bigg(\frac{60m_c^2Q^2y(1-y)(1-z)}{z}-\frac{26m_c^4(1-y)}{z^2}\\
&-\frac{26Q^4x(1-x)y(1-y)^3(1-z)^3}{z}\Bigg)F(m_c,Q^2)^2\Bigg\}\mathrm{Log}[F(m_c,Q^2)],\\
\Pi^{GG}(Q^2) =& \frac{\langle g_s^2GG\rangle}{288\pi^6}\int_0^1 dx\int_0^1 dy\int_0^1 dz\Bigg\{\left(\frac{30m_c^2x(1-x)(1-y)^3(1-z)^3}{z^3}-\frac{13m_c^2x(1-x)y(1-y)^3(1-z)^4}{z^3}\right)\\
&\times F(m_c,Q^2)+\Bigg(\frac{10m_c^4x(1-x)y(1-y)^3(1-z)^4}{z^3}-\frac{13m_c^4(1-y)(1-z)^2}{z^2}-\frac{10\mathrm{mc}^4(1-y)y(1-z)^3}{z^2}\\
&+\frac{15m_c^2Q^2(1-x)x(1-y)^3(1-z)^4}{z^2}-\frac{26m_c^2Q^2(1-x)x(1-y)^3(1-z)^5}{z^2}\Bigg)\Bigg\}\mathrm{Log}[F(m_c,Q^2)]\\
&+\frac{\langle g_s^2GG\rangle}{864\pi^6}\int_0^1 dx\int_0^1 dy\int_0^1 dz\frac{-1}{F(m_c,Q^2)}\Bigg\{\frac{13m_c^6(1-y)(1-z)^3}{z^2}-\frac{15m_c^4Q^2y(1-y)(1-z)^4}{z^2}\\
&-\frac{15m_c^2Q^2x(1-x)(1-y)^3(1-z)^5}{z^2}+\frac{13m_c^2Q^4x(1-x)y(1-y)^3(1-z)^6}{z}\Bigg\}\\
&+\frac{\langle g_s^2GG\rangle}{1152\pi^6}\int_0^1 dx\int_0^1 dy\int_0^1 dz\Bigg\{\left(\frac{18(1-x)x(1-y)^3(1-z)^2}{z^2}\right)F(m_c,Q^2)^2+\Bigg(\frac{-12m_c^2(1-y)(1-z)}{z}\\
&-\frac{14m_c^2x(1-x)(1-y)^3(1-z)^2}{yz^2}-\frac{24m_c^2y(1-z)}{xz}+\frac{36Q^2x(1-x)(1-y)^3(1-z)^3}{z}\Bigg)F(m_c,Q^2)\\
&+\Bigg(\frac{12m_c^4(1-y)(1-z)}{yz}-\frac{12m_c^2Q^2y(1-z)^2}{x}-6m_c^2Q^2(1-y)(1-z)^2\\
&-\frac{7m_c^2Q^2(1-x)x(1-y)^3(1-z)^3}{yz}+6Q^4(1-x)x(1-y)^3(1-z)^4\Bigg)\Bigg\}\mathrm{Log}[F(m_c,Q^2)], \qquad (19)
\end{aligned}
$$

where $F(m_c,Q^2)=m_c^2(1-z+\frac{z}{y}+\frac{z}{x(1-y)}+\frac{z}{(1-x)(1-y)})+Q^2z(1-z)$. We shall not evaluate the dimension-6 trigluon condensate $\langle G^3\rangle$ ($\sim g_s^3$) and dimension-8 $\langle G^4\rangle$ ($\sim g_s^4$) condensate in the OPE series. The $\langle G^3\rangle$ term gives negligible contribution to the correlation functions even at $\xi=0$ for the charmonium system [87] and four-charm tetraquark system [55]. For the dimension-8 $\langle G^4\rangle$ condensate, it was proven in the charmonium moment sum rules that this term was much larger suppressed comparing to the dimension-4 gluon condensate $\langle G^2\rangle$ at $\xi\neq 0$ and, thus, can also be neglected for the mass sum rule analysis [81,88].

To obtain convergent OPE series, we require that the contribution of the gluon condensate be smaller than the perturbative term and obtain the upper bound $n_{\max}=47$, 61, 77, 91 for $\xi=2,3,4,5$, respectively. We show the ratio $|\Pi^{GG}/\Pi^{\mathrm{Pert}}|$ in Fig. 1 to display the convergence of the OPE series with respect to n and ξ, which indicates that the OPE convergence becomes better with increasing of ξ and decreasing of n.

In Fig. 2, we show the variation of the extracted mass with n for different values of ξ and get stable mass prediction plateaus $(n,\xi)=(32,2),(42,3),(52,4),(62,5)$. To choose the values of ξ, one should consider both the existence of the mass plateaus and the stability of the hadron mass for growing ξ. Both of these criteria can be satisfied for $\xi\geq 2$, as shown in Fig. 2. Accordingly, the mass of such a $c\bar{c}c\bar{c}$ tetraquark state is finally predicted to be

$$
m_{c\bar{c}c\bar{c}}=6.54^{+0.19}_{-0.18}\ \mathrm{GeV}, \qquad (20)
$$

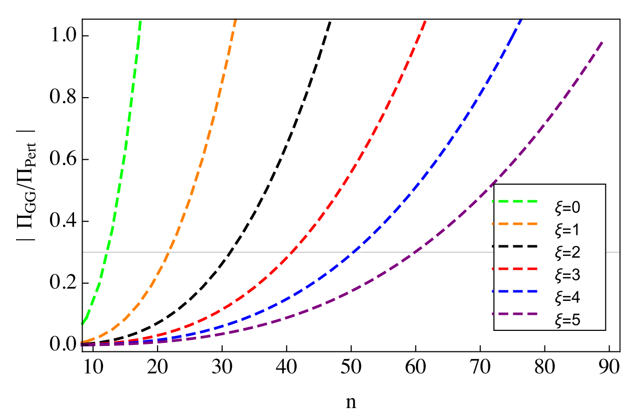

FIG. 1. $|\Pi^{GG}/\Pi^{\mathrm{Pert}}|$ with respect to n for different values of ξ from $J_1(x)$ with $J^{PC}=0^{++}$.

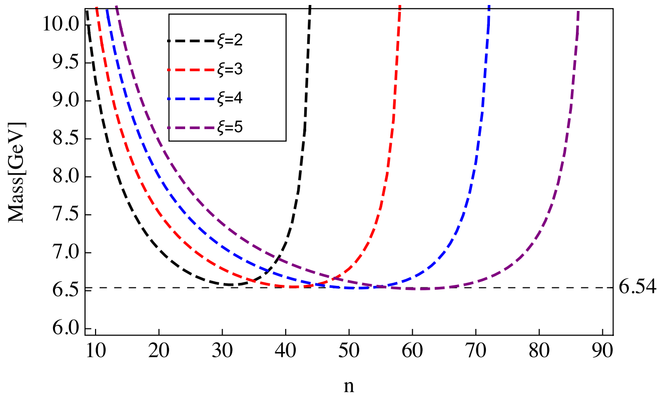

FIG. 2. Hadron mass for the fully charm $c\bar{c}c\bar{c}$ tetraquark state with $J^{PC} = 0^{++}$ from $J_1(x)$ with respect to n for different values of ξ.

in which the errors come from the uncertainties of ξ and n, charm quark mass, and the gluon condensate.

The same numerical analyses can be done for the other interpolating currents in Eqs. (2) and (3). Then we obtain the masses for all $c\bar{c}c\bar{c}$ tetraquark states in $\mathbf{8}_{[c\bar{c}]} \otimes \mathbf{8}_{[c\bar{c}]}$ configuration in Table I. In this mass spectra, we predict three S-wave $c\bar{c}c\bar{c}$ tetraquarks with $J^{PC} = 0^{++}$, 1^{+-}, and 2^{++} and four P-wave $c\bar{c}c\bar{c}$ tetraquarks with $J^{PC} = 0^{-+}$, 0^{--}, 1^{--}, and 1^{-+}. The masses are predicted to be around 6.3–6.5 GeV for the S-wave states while 7.0–7.2 GeV for the P-wave states. Comparing to the mass spectra obtained in Ref. [23], the masses for S-wave fully charm tetraquark states are consistent with each other in both the $[c\bar{c}][c\bar{c}]$ and $[cc][\bar{c}\bar{c}]$ configurations. However, the P-wave $[c\bar{c}][c\bar{c}]$ tetraquarks are predicted to be 200–300 MeV higher than those in the diquark-antidiquark configuration [23]. In Table I, we also list the masses for some S-wave $c\bar{c}c\bar{c}$ tetraquark states in $\mathbf{8}_{[c\bar{c}]} \otimes \mathbf{8}_{[c\bar{c}]}$ configuration obtained by the Laplace QCD sum rule [54] and a nonrelativistic quark model [61]. Our results for these $c\bar{c}c\bar{c}$ tetraquark states are in good agreement with those in Refs. [54,61].

TABLE I. The mass spectra for the fully charm $c\bar{c}c\bar{c}$ tetraquark states in $\mathbf{8}_{[c\bar{c}]} \otimes \mathbf{8}_{[c\bar{c}]}$ color configuration.

Current	J^{PC}	Mass (GeV)	Reference [54] (GeV)	Reference [61] (MeV)
J_1	0^{++}	$6.54^{+0.19}_{-0.18}$	$6.44^{+0.11}_{-0.11}$	6403
J_2	0^{++}	$6.36^{+0.16}_{-0.16}$	$6.52^{+0.11}_{-0.11}$	6346
$J_{1\mu}$	1^{+-}	$6.47^{+0.18}_{-0.17}$	...	6325
$J_{\mu\nu}$	2^{++}	$6.52^{+0.17}_{-0.17}$	...	6388
η_1	0^{-+}	$7.00^{+0.23}_{-0.20}$	...	...
η_2	0^{-+}	$7.02^{+0.24}_{-0.20}$	...	...
η_3	0^{--}	$7.00^{+0.23}_{-0.20}$	...	...
$\eta_{1\mu}$	1^{--}	$6.99^{+0.23}_{-0.20}$	...	...
$\eta_{2\mu}$	1^{--}	$7.17^{+0.28}_{-0.22}$	...	...
$\eta_{3\mu}$	1^{-+}	$6.98^{+0.21}_{-0.19}$	...	...
$\eta_{4\mu}$	1^{-+}	$7.07^{+0.21}_{-0.19}$	...	...

One notes that the two interpolating currents in the same channel ($J^{PC} = 0^{++}, 0^{-+}, 1^{-+}, 1^{--}$) lead to almost the same hadron masses. To specify if these two currents couple to the same physical state or not, we calculate their cross-correlation functions of two different currents with the same quantum number, e.g., the $J_1(x)$ and $J_2(x)$ with $J^{PC} = 0^{++}$:

$$\Pi_{12}(p^2) = i \int d^4x e^{ip\cdot x} \langle 0|T[J_1(x)J_2^\dagger(0)]|0\rangle. \quad (21)$$

Our calculations show that all these cross-correlation functions are large enough and comparable to the diagonal correlators, implying that they couple to the same physical states. Since the two interpolating currents in the same channel give almost the same hadron masses, we do not reanalyze the mass sum rules by using their mixing current, avoiding more errors from the uncertain mixing angle.

We can also study the fully bottom tetraquark states in $\mathbf{8}_{[b\bar{b}]} \otimes \mathbf{8}_{[b\bar{b}]}$ configuration. For the fully bottom system, we define $\xi = Q_0^2/(m_b)^2$ and find that the two criteria of mass plateaus and ξ stability can be achieved for $\xi = 0.2$–0.8. By requiring that the contribution of the gluon condensate be smaller than the perturbative term, we obtain the upper bound on the parameter $n_{\max} = 119$, 121, 123, 125 for $\xi = 0.2$, 0.4, 0.6, 0.8, respectively. We show the variation of the extracted mass with n for different value of ξ in Fig. 3 and get stable mass prediction plateaus $(n, \xi) = (75, 0.2), (77, 0.4), (77, 0.6), (79, 0.8)$. The mass of such a $b\bar{b}b\bar{b}$ tetraquark state is finally predicted as

$$m_{b\bar{b}b\bar{b}} = 18.15^{+0.14}_{-0.10}\ \text{GeV}. \quad (22)$$

Applying a similar moment sum rule analyses, we obtain the mass spectra for these $b\bar{b}b\bar{b}$ tetraquark states and list them in Table II. Accordingly, the S-wave $b\bar{b}b\bar{b}$ tetraquark

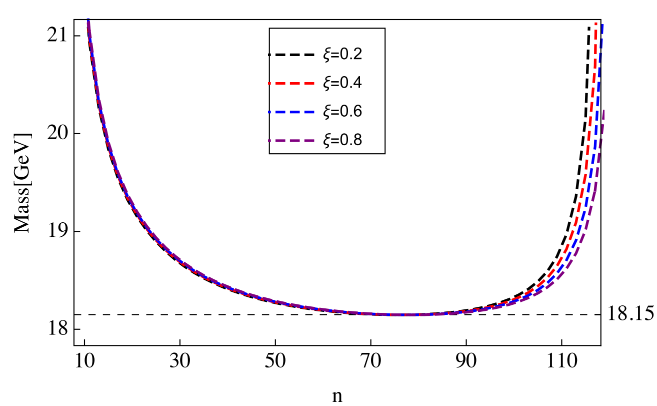

FIG. 3. Hadron mass for fully bottom $b\bar{b}b\bar{b}$ tetraquark state with $J^{PC} = 0^{++}$ from $J_1(x)$ with respect to n for different values of ξ.

TABLE II. The mass spectra for the fully bottom $b\bar{b}b\bar{b}$ tetraquark states in $\mathbf{8}_{[b\bar{b}]} \otimes \mathbf{8}_{[b\bar{b}]}$ color configuration.

Current	J^{PC}	Mass (GeV)	Reference [54] (GeV)	Reference [61] (MeV)
J_1	0^{++}	$18.15^{+0.14}_{-0.10}$	$18.38^{+0.11}_{-0.11}$	19243
J_2	0^{++}	$18.13^{+0.13}_{-0.09}$	$18.44^{+0.10}_{-0.10}$	19237
$J_{1\mu}$	1^{+-}	$18.14^{+0.14}_{-0.09}$	⋯	19126
$J_{\mu\nu}$	2^{++}	$18.15^{+0.14}_{-0.09}$	⋯	19197
η_1	0^{-+}	$18.45^{+0.15}_{-0.11}$	⋯	⋯
η_2	0^{-+}	$18.54^{+0.16}_{-0.12}$	⋯	⋯
η_3	0^{--}	$18.47^{+0.15}_{-0.11}$	⋯	⋯
$\eta_{1\mu}$	1^{--}	$18.46^{+0.15}_{-0.11}$	⋯	⋯
$\eta_{2\mu}$	1^{--}	$18.46^{+0.15}_{-0.11}$	⋯	⋯
$\eta_{3\mu}$	1^{-+}	$18.56^{+0.16}_{-0.11}$	⋯	⋯
$\eta_{4\mu}$	1^{-+}	$18.79^{+0.18}_{-0.13}$	⋯	⋯

states are obtained to be around 18.2 GeV, while the P-wave states are about 18.4–18.8 GeV. Such results are several hundreds of MeV below the masses of diquark-antidiquark $bb\bar{b}\bar{b}$ tetraquarks predicted in Ref. [23]. As shown in Table II, our results for the S-wave $\mathbf{8}_{[b\bar{b}]} \otimes \mathbf{8}_{[b\bar{b}]}$ tetraquarks are much smaller than those predicted in the nonrelativistic quark model [61] but roughly in agreement with the results in Laplace QCD sum rules [54].

V. CONCLUSION AND DISCUSSION

We have studied the fully heavy $Q\bar{Q}Q\bar{Q}$ tetraquark states in the $\mathbf{8}_{[Q\bar{Q}]} \otimes \mathbf{8}_{[Q\bar{Q}]}$ color structure by using the moment QCD sum rule method. We construct the S-wave and P-wave interpolating tetraquark currents with various quantum numbers and calculate their two-point correlation functions containing a perturbative term and a gluon condensate term. Choosing suitable parameter working regions, we have established stable moment sum rules for all interpolating currents and extracted the mass spectra for the fully charm and fully bottom tetraquark states.

For the fully charm $c\bar{c}c\bar{c}$ system, our results suggest that the S-wave tetraquark states with $J^{PC} = 0^{++}, 1^{+-}, 2^{++}$ lie around 6.3–6.5 GeV, while the P-wave tetraquark states with $J^{PC} = 0^{-+}, 0^{--}, 1^{--}, 1^{-+}$ are about 7.0–7.2 GeV. Especially, the masses for the $c\bar{c}c\bar{c}$ tetraquarks with $J^{PC} = 0^{++}$ and 2^{++} are consistent with the broad structure observed by LHCb [33]. The P-wave fully charm tetraquarks with $J^{PC} = 0^{-+}$ and 1^{-+} are predicted to be roughly in agreement with the mass of $X(6900)$ within errors. Such results suggest the possibility that there are some $\mathbf{8}_{[c\bar{c}]} \otimes \mathbf{8}_{[c\bar{c}]}$ components in LHCb's di-J/ψ structures. More investigations are needed in both theoretical and experimental aspects to study the nature of these structures.

For the fully bottom $b\bar{b}b\bar{b}$ system, the numerical results show that the S-wave tetraquark states are about 18.2 GeV, while the P-wave states are around 18.4–18.8 GeV. All these fully bottom $b\bar{b}b\bar{b}$ tetraquarks are predicted to be below the $\eta_b\eta_b$ and $\Upsilon(1S)\Upsilon(1S)$ two-meson decay thresholds, indicating that these tetraquark states will be stable against the strong interaction. Such results are consistent with our previous prediction for the diquark-antidiquark $bb\bar{b}\bar{b}$ tetraquarks in Ref. [23]. More efforts are expected to search for such fully bottom tetraquark states in the future experiments, such as LHCb, CMS, and so on.

ACKNOWLEDGMENTS

This work is supported by the National Natural Science Foundation of China under Grant No. 12175318 and the National Key R&D Program of China under Contract No. 2020YFA0406400.

[1] M. Gell-Mann, Phys. Lett. **8**, 214 (1964).
[2] G. Zweig, CERN Report No. 8419 TH 412, 1964 (unpublished); reprinted in *Developments in the Quark Theory of Hadrons*, edited by D. B. Lichtenberg and S. P. Rosen (Hadronic Press, Massachusetts, 1980).
[3] S.-K. Choi *et al.*, Phys. Rev. Lett. **91**, 262001 (2003).
[4] M. Ablikim *et al.*, Phys. Rev. Lett. **112**, 132001 (2014).
[5] M. Ablikim *et al.*, Phys. Rev. Lett. **110**, 252001 (2013).
[6] B. Aubert *et al.*, Phys. Rev. Lett. **95**, 142001 (2005).
[7] B. Aubert *et al.*, Phys. Rev. Lett. **98**, 212001 (2007).
[8] A. Bondar *et al.*, Phys. Rev. Lett. **108**, 122001 (2012).
[9] X. L. Wang *et al.*, Phys. Rev. Lett. **99**, 142002 (2007).
[10] R. Aaij *et al.*, Phys. Rev. Lett. **115**, 072001 (2015).
[11] R. Aaij *et al.*, Phys. Rev. Lett. **122**, 222001 (2019).
[12] R. Aaij *et al.*, Sci. Bull. **66**, 1278 (2021).
[13] H.-X. Chen, W. Chen, X. Liu, and S.-L. Zhu, Phys. Rep. **639**, 1 (2016).
[14] A. Ali, J. S. Lange, and S. Stone, Prog. Part. Nucl. Phys. **97**, 123 (2017).
[15] R. F. Lebed, R. E. Mitchell, and E. S. Swanson, Prog. Part. Nucl. Phys. **93**, 143 (2017).
[16] F.-K. Guo, C. Hanhart, U.-G. Meißner, Q. Wang, Q. Zhao, and B.-S. Zou, Rev. Mod. Phys. **90**, 015004 (2018).
[17] Y.-R. Liu, H.-X. Chen, W. Chen, X. Liu, and S.-L. Zhu, Prog. Part. Nucl. Phys. **107**, 237 (2019).
[18] N. Brambilla, S. Eidelman, C. Hanhart, A. Nefediev, C.-P. Shen, C. E. Thomas, A. Vairo, and C.-Z. Yuan, Phys. Rep. **873**, 1 (2020).
[19] V. Khachatryan *et al.*, J. High Energy Phys. 05 (2017) 013.
[20] L. C. Bland *et al.*, arXiv:1909.03124.

[21] R. Aaij *et al.*, J. High Energy Phys. 10 (2018) 086.
[22] A. Sirunyan *et al.*, Phys. Lett. B **808**, 135578 (2020).
[23] W. Chen, H.-X. Chen, X. Liu, T. G. Steele, and S.-L. Zhu, Phys. Lett. B **773**, 247 (2017).
[24] M. N. Anwar, J. Ferretti, F.-K. Guo, E. Santopinto, and B.-S. Zou, Eur. Phys. J. C **78**, 647 (2018).
[25] A. Esposito and A. D. Polosa, Eur. Phys. J. C **78**, 782 (2018).
[26] C. Hughes, E. Eichten, and C. T. H. Davies, Phys. Rev. D **97**, 054505 (2018).
[27] M. Karliner, S. Nussinov, and J. L. Rosner, Phys. Rev. D **95**, 034011 (2017).
[28] J. Wu, Y.-R. Liu, K. Chen, X. Liu, and S.-L. Zhu, Phys. Rev. D **97**, 094015 (2018).
[29] J.-M. Richard, A. Valcarce, and J. Vijande, Phys. Rev. D **95**, 054019 (2017).
[30] Y. Bai, S. Lu, and J. Osborne, Phys. Lett. B **798**, 134930 (2019).
[31] X.-Y. Chen, Eur. Phys. J. A **55**, 106 (2019).
[32] V. R. Debastiani and F. S. Navarra, Chin. Phys. C **43**, 013105 (2019).
[33] R. Aaij *et al.*, Sci. Bull. **65**, 1983 (2020).
[34] R. Albuquerque, S. Narison, A. Rabemananjara, D. Rabetiarivony, and G. Randriamanatrika, Phys. Rev. D **102**, 094001 (2020).
[35] J. F. Giron and R. F. Lebed, Phys. Rev. D **102**, 074003 (2020).
[36] M. C. Gordillo, F. De Soto, and J. Segovia, Phys. Rev. D **102**, 114007 (2020).
[37] Z.-H. Guo and J. A. Oller, Phys. Rev. D **103**, 034024 (2021).
[38] X. Jin, Y. Xue, H. Huang, and J. Ping, Eur. Phys. J. C **80**, 1083 (2020).
[39] M. Karliner and J. L. Rosner, Phys. Rev. D **102**, 114039 (2020).
[40] H.-W. Ke, X. Han, X.-H. Liu, and Y.-L. Shi, Eur. Phys. J. C **81**, 427 (2021).
[41] Q. Li, C.-H. Chang, G.-L. Wang, and T. Wang, Phys. Rev. D **104**, 014018 (2021).
[42] Z.-R. Liang, X.-Y. Wu, and D.-L. Yao, Phys. Rev. D **104**, 034034 (2021).
[43] M.-S. Liu, Q.-F. Lü, X.-H. Zhong, and Q. Zhao, Phys. Rev. D **100**, 016006 (2019).
[44] M.-S. Liu, F.-X. Liu, X.-H. Zhong, and Q. Zhao, arXiv: 2006.11952.
[45] S. Pal, R. Ghosh, B. Chakrabarti, and A. Bhattacharya, Eur. Phys. J. Plus **136**, 625 (2021).
[46] J. Sonnenschein and D. Weissman, Eur. Phys. J. C **81**, 25 (2021).
[47] B.-D. Wan and C.-F. Qiao, Phys. Lett. B **817**, 136339 (2021).
[48] Z.-G. Wang and Z.-Y. Di, Acta Phys. Pol. B **50**, 1335 (2019).
[49] G.-J. Wang, L. Meng, and S.-L. Zhu, Phys. Rev. D **100**, 096013 (2019).
[50] Z.-G. Wang, Chin. Phys. C **44**, 113106 (2020).
[51] G.-J. Wang, L. Meng, M. Oka, and S.-L. Zhu, Phys. Rev. D **104**, 036016 (2021).
[52] X.-Z. Weng, X.-L. Chen, W.-Z. Deng, and S.-L. Zhu, Phys. Rev. D **103**, 034001 (2021).
[53] G. Yang, J.-L. Ping, L.-Y. He, and Q. Wang, arXiv:2006.13756.
[54] B.-C. Yang, L. Tang, and C.-F. Qiao, Eur. Phys. J. C **81**, 324 (2021).
[55] J.-R. Zhang, Phys. Rev. D **103**, 014018 (2021).
[56] Z. Zhao, K. Xu, A. Kaewsnod, X. Liu, A. Limphirat, and Y. Yan, Phys. Rev. D **103**, 116027 (2021).
[57] J. Zhao, S. Shi, and P. Zhuang, Phys. Rev. D **102**, 114001 (2020).
[58] R. Zhu, Nucl. Phys. **B966**, 115393 (2021).
[59] Q.-F. Cao, H. Chen, H.-R. Qi, and H.-Q. Zheng, Chin. Phys. C **45**, 103102 (2021).
[60] H. Mutuk, Eur. Phys. J. C **81**, 367 (2021).
[61] G. Yang, J. Ping, and J. Segovia, Phys. Rev. D **104**, 014006 (2021).
[62] Y. Huang, F. Feng, Y. Jia, W.-L. Sang, D.-S. Yang, and J.-Y. Zhang, Chin. Phys. C **45**, 093101 (2021).
[63] F. Feng, Y. Huang, Y. Jia, W.-L. Sang, X. Xiong, and J.-Y. Zhang, arXiv:2009.08450.
[64] X.-Y. Wang, Q.-Y. Lin, H. Xu, Y.-P. Xie, Y. Huang, and X. Chen, Phys. Rev. D **102**, 116014 (2020).
[65] F. Feng, Y. Huang, Y. Jia, W.-L. Sang, and J.-Y. Zhang, Phys. Lett. B **818**, 136368 (2021).
[66] R. Maciuła, W. Schäfer, and A. Szczurek, Phys. Lett. B **812**, 136010 (2021).
[67] V. P. Gonçalves and B. D. Moreira, Phys. Lett. B **816**, 136249 (2021).
[68] Y.-Q. Ma and H.-F. Zhang, arXiv:2009.08376.
[69] J.-Z. Wang, X. Liu, and T. Matsuki, Phys. Lett. B **816**, 136209 (2021).
[70] J.-W. Zhu, X.-D. Guo, R.-Y. Zhang, W.-G. Ma, and X.-Q. Li, arXiv:2011.07799.
[71] C. Gong, M.-C. Du, B. Zhou, Q. Zhao, and X.-H. Zhong, Phys. Lett. B **824**, 136794 (2022).
[72] Q.-F. Lü, D.-Y. Chen, and Y.-B. Dong, Eur. Phys. J. C **80**, 871 (2020).
[73] G. Li, X.-F. Wang, and Y. Xing, Eur. Phys. J. C **79**, 645 (2019).
[74] H.-X. Chen, W. Chen, X. Liu, and S.-L. Zhu, Sci. Bull. **65**, 1994 (2020).
[75] C. Becchi, J. Ferretti, A. Giachino, L. Maiani, and E. Santopinto, Phys. Lett. B **811**, 135952 (2020).
[76] L. Maiani, Sci. Bull. **65**, 1949 (2020).
[77] K.-T. Chao and S.-L. Zhu, Sci. Bull. **65**, 1952 (2020).
[78] X.-K. Dong, V. Baru, F.-K. Guo, C. Hanhart, A. Nefediev, and B.-S. Zou, Sci. Bull. **66**, 2462 (2021).
[79] Z.-Y. Yang, Q.-N. Wang, W. Chen, and H.-X. Chen, Phys. Rev. D **104**, 014003 (2021).
[80] Q.-N. Wang, Z.-Y. Yang, W. Chen, and H.-X. Chen, Phys. Rev. D **104**, 014020 (2021).
[81] L. Reinders, H. Rubinstein, and S. Yazaki, Phys. Rep. **127**, 1 (1985).
[82] M. Shifman, A. Vainshtein, and V. Zakharov, Nucl. Phys. **B147**, 385 (1979).
[83] W. Chen, T. G. Steele, H.-X. Chen, and S.-L. Zhu, Phys. Rev. D **92**, 054002 (2015).
[84] M. Nielsen, F. S. Navarra, and S. H. Lee, Phys. Rep. **497**, 41 (2010).
[85] S. Narison, Nucl. Part. Phys. Proc. **300–302**, 153 (2018).
[86] P. Zyla *et al.*, Prog. Theor. Exp. Phys. **2020**, 083C01 (2020).
[87] S. N. Nikolaev and A. V. Radyushkin, Phys. Lett. **110B**, 476 (1982); Nucl. Phys. **B213**, 285 (1983).
[88] S. N. Nikolaev and A. V. Radyushkin, Phys. Lett. **124B**, 243 (1983).